Hindawi
Journal of Nanomaterials
Volume 2017, Article ID 8290892, 13 pages
https://doi.org/10.1155/2017/8290892

*Research Article*

# Preparation and Characterization of Pd Modified $TiO_2$ Nanofiber Catalyst for Carbon–Carbon Coupling Heck Reaction

**Leah O. Nyangasi,[1,2] Dickson M. Andala,[3] Charles O. Onindo,[1] Jane C. Ngila,[4] Banothile C. E. Makhubela,[5] and Eric M. Ngigi[4]**

[1]*Chemistry Department, Kenyatta University, P.O. Box 43844-00100, Nairobi, Kenya*
[2]*Natural Science Department, Catholic University of Eastern Africa, P.O. Box 62157-00200, Nairobi, Kenya*
[3]*Chemistry Department, Multimedia University of Kenya, P.O. Box 30305-00100, Nairobi, Kenya*
[4]*Department of Applied Chemistry, University of Johannesburg, P.O. Box 17011, Corner Beit and Nind Street, Doornfontein, Johannesburg 2028, South Africa*
[5]*Department of Chemistry, University of Johannesburg, P.O. Box 17011, Kingsway Campus, Auckland Park 2006, South Africa*

Correspondence should be addressed to Leah O. Nyangasi; lnyangasi@gmail.com

Received 27 June 2017; Revised 12 September 2017; Accepted 12 October 2017; Published 9 November 2017

Academic Editor: Sherine Obare



$TiO_2$ fibers were prepared through electrospinning of poly methyl methacrylate (PMMA) and titanium isopropoxide (TIP) solution followed by calcination of fibers in air at 500°C. Cetyltrimethylammonium bromide (CTAB) protected palladium nanoparticles (Pd NPs) prepared through reduction method were successfully adsorbed on the $TiO_2$ nanofibers (NF). Combined studies of X-ray diffraction (XRD), scanning electron microscope (SEM), and transmission electron microscope (TEM) indicated that the synthesized Pd/$TiO_2$ had anatase. BET indicated that the synthesized $TiO_2$ and Pd/$TiO_2$ had a surface area of 53.4 and 43.4 $m^2/g$, respectively. The activity and selectivity of 1 mol% Pd/$TiO_2$ in the Heck reaction have been investigated towards the Mizoroki-Heck carbon–carbon cross-coupling of bromobenzene (ArBr) and styrene. Temperature, time, solvent, and base were optimized and catalyst was recycled thrice. $^1$H NMR and $^{13}$C NMR indicated that stilbene, a known compound from literature, was obtained in various Heck reactions at temperatures between 100°C and 140°C but the recyclability was limited due to some palladium leaching and catalyst poisoning which probably arose from some residual carbon from the polymer. The catalyst was found to be highly active under air atmosphere with reaction temperatures up to 140°C. Optimized reaction condition resulted in 89.7% conversions with a TON of 1993.4 and TOF value of 332.2 $hr^{-1}$.

## 1. Introduction

The Heck coupling reaction (HR) is a single operational step reaction involving an aryl halide and an olefin (Scheme 1), in the presence of palladium catalyst, a solvent, and a base. HR can be used to produce fine chemicals such as detergents, plastics, pharmaceuticals, and polymers [1–4]. The herbicide Prosulfuron™, the sunscreen agent 2-ethylhexyl p-methoxycinnamate, and Naproxen™, antiasthma agent Singulair™, are examples of compounds that have been produced on large scale [1]. 1–5% mole palladium species has commonly been used in homogenous system with palladium being generated by $Pd^{2+}$ salts with ligands such as $Cl^-$, $PPh_3$, dba, N-heterocyclic carbenes [5, 6], phosphorus and/or oxygen based ligands [1, 7], thiosemicarbazones [7], and bis(thio)urea ligands [8] in the presence of organic and/or inorganic bases for neutralization of the reaction.

Homogenous catalysis efficiency has been limited by formation of black palladium precipitate, unstable catalysts, nonrecyclability of the catalyst, and use of expensive and hazardous reagents all leading to low percentage yields [1, 2, 5, 8]. To help address the problem of recovery and recycling

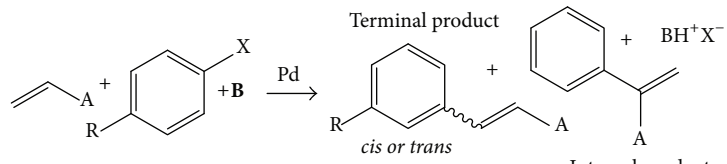


A: Ph, OR, COOR, CONR′CN...
X: Halide, $OSO_2CF_3$, $COCl_2$ ...
R: H, alkyl, COR′COH, $NO_2$, Halide... (o, p, m)
B: $M_2CO_3$, MOAc (M: alkali metal), $K_3PO_4$, $NR'_3$ ...

Scheme 1: General Heck reaction.

of the catalyst, different support materials have been and are still being investigated. The most attractive is Pd on carbon or carbon nanotubes [9–11]: Pd on metal oxide such as MgO, $Al_2O_3$, ZnO, $ZrO_2$, and $TiO_2$ [5, 12–15], Pd on zeolites [16], Pd encapsulated in large organic structures (dendrimers) [17], and Pd on block copolymer micelles [18]. The supports tend to arrest Pd on the surface of a solid material or in an organic matrix, making it possible to stabilize the catalytically active palladium species and prevent sintering.

Metal oxides have become the most lucrative Pd supports for heterogeneous catalysis due to their availability, low production costs, and photoinduced electron hole pairs on the surfaces of metal oxide which can be harvested to enhance electron transfer and their chemical reactivity [22, 23]. The first paper on heterogenous Heck catalysis of Pd supported on an inorganic support was reported in 1990 [19, 21], reporting the coupling of chlorobenzene and styrene in the presence of Pd/MgO, methanol solvent, and sodium carbonate as a base at 150°C. Several other reports have since been made and Table 1 summarizes the literature on metal oxide support and Heck reaction.

Titania, a semiconductor, has attracted more research interest due to its large band gap ~3.0–3.2 eV. From literature, $Pd/TiO_2$ catalyst for HR was previously prepared by impregnation of Titania followed by hydrogen reduction of palladium precursor. In 2011, Obuya and coworkers photodeposited Pd NPs of diameters within 2–5 nm on electrospun $TiO_2$ NF. In 2014, Nasrollahzadeh and his group dispersed 40 nm Pd NPs on commercial $TiO_2$ using simple drop drying process. The catalyst was used in ArI-styrene system at 140°C for 10 h. In a different method, Li and his team synthesized $Pd/TiO_2$ through adsorption method by pH control and applied it in the Heck system of and methyl acrylate in the presence of 0.1–0.5% $Pd/TiO_2$ catalyst and KOAc base and DMA solvent [12]. Generally, the reported results by the separate groups showed variation in products yield. This could probably be attributed to variation in bases and solvents used, percentage mole of palladium, and the method of preparing the support. The method of synthesizing Pd NPs for C-C coupling reactions has also remained an area of interest [5].

This paper reports a simple and inexpensive method for preparation of heterogenous and reusable $Pd/TiO_2$ through electrospinning to produce high surface area fibers followed by palladium deposition-reduction. The efficiency of the synthesized catalyst was evaluated in a styrene-ArBr model Heck C-C coupling reaction.

## 2. Experimental Methods

*2.1. Materials.* The synthesis and reactions were carried out using commercially available reagents. Poly methyl methacrylate (PMMA) Mw 996,000 by GPC crystalline, titanium isopropoxide (TIP), sodium acetate (NaOAc), bromobenzene (ArBr), styrene (99.0%), hydrazine monohydrate ($N_2H_4$ 64-65% reagent grade (98%), palladium acetylacetonate ($Pd(acac)_2$) (99.9%), dimethyl formamide (DMF), ethanol 99.8%, and methyl acrylate (99%) were purchased from Sigma and Aldrich. Anhydrous sodium carbonate ($Na_2CO_3$) 99.5% was purchased from Promark Chemicals. Cetyltrimethylammonium bromide (CTAB), Molecular Biology Grade (99.0%), was purchased from Calbiochem®. All chemicals were used without any further purification.

*2.2. Structural Characterizations of Catalyst.* The morphology of the nanoparticles of $TiO_2$ and $Pd/TiO_2$ was observed using a scanning electron microscope (SEM, Tescan, Japan) at an accelerated voltage of 20 kV. Prior to scanning by electron microscope, the samples were sputter-coated with carbon using a Jeol JFC-1200 fine coater. Elemental analysis or chemical characterization was done by X-ray powder diffractometer (XRD PANalytical X-Pert diffractometer with Cu-K$\alpha$ radiation 1.54060 Å; PANalytical BV, Netherlands). Brunauer–Emmett–Teller (BET) surface areas of the powders were determined by nitrogen adsorption at –196°C in the range of a relative pressure $P/P^0$ from 0.05 to 1. Samples were degaussed at 120°C for 7 h prior to nitrogen adsorption measurements. The surface area and pore size were analyzed on micromeritics ASAP 2020. The pore size distributions were obtained from the desorption branch of the isotherm using the Barret-Joyner-Halenda (BJH) procedure. TEM images were taken using JOEL, JEM 2100 Transmission Emission Microscope (TEM). The samples were sonicated in ethanol, placed on a copper grid, and left in the air for the solvent to evaporate. IR spectra were recorded on Perkin–Elmer 100 spectrophotometer FTIR series (Tokyo, Japan) measured as KBr pellets (1 : 10, sample/KBr). The instrument was set to scan from 400 $cm^{-1}$ to 4000 $cm^{-1}$ and the spectra were obtained. Concentrations of styrene and ArBr in the Heck reaction were determined using a Varian 3900 GC model, Netherlands, with a flame ionization detector (FID) and a Megabore column (length 25 m with 0.23 mm i.d.). The programme ran from 80°C to 240°C at a flow of 1.0 mL per min and a velocity of 24 cm $min^{-1}$.

Table 1: Selected Heck reaction of palladium supported on inorganic oxides.

| Catalyst | ArX | Alkene | Base | ArX/alkene/base/Pd Mol/mol/mol/mol | Solvent | $T$ °C | Time h | Yield% | Selectivity Reg | Selectivity Chemo | Ref |
|---|---|---|---|---|---|---|---|---|---|---|---|
| Pd/MgO | ArCl | Styrene | $Na_2CO_3$ | $7/1/0.33/2 \times 10^{-4}$ | Methanol | 150 | 5 | 32 | 42 | | [19] |
| Pd/$Al_2O_3$ 6.06% | 4-Nitrobenzoyl chloride | VBA | $Et_3N$ | $1/2/1.2/2.5 \times 10^{-3}$ | Dioxane | 100 | 4 | 71 | 10 | 3.9 | [20] |
| Pd/$SiO_2$ 1.22% | 4-Nitrobenzoyl chloride | VBAr | $Et_3N$ | $1/2/1.2/2.5 \times 10^{-3}$ | Dioxane | 100 | 4 | 51 | 10 | 3.2 | [20] |
| Pd/$Al_2O_3$ 5% | ArI | Acrylonitrile | $Et_3N$ | $1/1/1/1 \times 10^{-2}$ | Acetonitrile | 140 | 14 | 72 | 3.3 | 20 | [21] |
| Pd/MgO 5% | ArI | Acrylonitrile | $Et_3N$ | $1/1/1/1 \times 10^{-2}$ | Acetonitrile | 140 | 14 | 78 | 3.5 | 10 | [21] |
| Pd/MgO 5% | ArBr | Styrene | NaOAc | $1/1.5/1.2/1 \times 10^{-3}$ | DMA | 140 | 20 | 36.5 | 12.5 | 112 | [14] |
| Pd/ZnO 4.5% | ArBr | Styrene | NaOAc | $1/1.5/1.2/1 \times 10^{-3}$ | DMA | 140 | 20 | 33.3 | 11.8 | 101 | [14] |
| Pd/$TiO_2$ 4.3% | ArBr | Styrene | NaOAc | $1/1.5/1.2/1 \times 10^{-3}$ | DMA | 140 | 20 | 41.2 | 12.7 | 95 | [14] |
| Pd/$ZrO_2$ 5.5% | ArBr | Styrene | NaOAc | $1/1.5/1.2/1 \times 10^{-3}$ | DMA | 140 | 20 | 49.1 | 12.3 | 112 | [14] |
| Pd/$TiO_2$ 1% | ArBr | Styrene | $Et_3N$ | 1/1.2/2/1.0 | DMF | 140 | 24 | 91 | | | [13] |
| Pd/$TiO_2$ 0.26% | ArBr | Methyl acrylate | KOAc | $0.5/0.6/0.6/5 \times 10^{-1}$ | DMA | 140 | 24 | 79 | | | [12] |
| Pd/$TiO_2$ 5% | ArI | Styrene | NaOAc | $4.44/6.69/7.23/5 \times 10^{-2}$ | NMP | 160 | | 90 | | | [22] |
| Pd/$TiO_2$ 1% | ArBr | Styrene | NaOAc | $1/1.2/2 \times 10^{-2}$ | DMF | 140 | 6 | 89.7 | | | This paper |
| Pd/$TiO_2$ 1% | ArBr | Methyl acrylate | NaOAc | $1/1.2/2 \times 10^{-2}$ | DMF | 140 | 6 | 80.6 | | | This paper |

$Et_3N$: triethylamine; ArBr: bromobenzene; ArI: iodobenzene; VBA: vinyl butyl ether; DMA: dimethylacetamide; NMP: N-methyl-2-pyrrolidone.

$^1$H and $^{13}$C NMR spectra were recorded on Bruker Magnetic system 400 MHz spectrometer at room temperature (298 K) equipped with a 5 mm BBO probe at the University of Johannesburg (400 MHz for $^1$H and 100 MHz for $^{13}$C). The $^1$H and $^{13}$C spectra were referenced internally using the residual $CDCl_3$ and reported relative to the internal standard tetramethylsilane (TMS) and chemical shift values given in ppm. Inductively coupled plasma-optical emission spectrometer (ICP-OES), Spectro Arcos (Germany), was used to quantify the amount of Pd in the catalyst after the reaction.

*2.3. Synthesis of $TiO_2$ Nanofibers.* 100 mg/mL of PMMA in 2 : 3 DCM/DMF was magnetically stirred until a homogenous solution was obtained. TIP was added to the polymer solution in the ratio of 1 : 2 (PMMA : TIP) and the mixture stirred for 10 minutes. The resulting PMMA/TIP solution was then electrospun, at 18 kV and 18 cm using electrospinning equipment model Holmarc's HO-NFES-040. The spun fibers were then allowed to stand for 4 h at room temperature to dry off the solvents and to allow the hydrolysis of titanium (IV) hydroxide, $Ti(OH)_4$, to go to completion. The dried material was then peeled off the aluminum foil and transferred to a ceramic boat for annealing in a Lindberg/Blue M, model number TF55035C-1 furnace. The fibers were annealed at 500°C for 3 h, in a continuous flow of air at a ramp rate of 10°C/min.

*2.4. Synthesis of Pd/$TiO_2$ Nanofibers.* CTAB protected and stabilized Pd NPs were prepared by modified Brust method [24]. 1.0 g of TIP and 1.1 g of CTAB were mixed with 40 mL of Toluene, sonicated for 20 minutes, transferred to a two-neck round bottomed flask, and refluxed at 40°C for 1 h. In a separate beaker 1% of $Pd(acac)_2$ with respect to TIP and 1.0 g of CTAB were dissolved in 20 mL of Toluene and sonicated for 30 minutes to make the precursor solution. Hydrazine monohydrate, $N_2H_4$ 60–65%, was added dropwise to reduce $Pd^{2+}$ to $Pd^0$ as shown in

$$2Pd^{2+} + 4OH^- + N_2H_4 \longrightarrow Pd^0 + N_2 + 4H_2O \quad (1)$$

The mixture turned from cream yellow to cream and finally formed a grey precipitate. The precipitate was immediately added to the $TiO_2$ solution and refluxed further for 1 h at 40°C.

The mixture was then cooled to room temperature and the sample dried overnight in an oven at 70°C. The dry sample was then washed with ethanol, water, and acetone to remove the organic materials. The cleaned sample was then calcined in air at 500°C for 3 h to obtain Pd/$TiO_2$.

*2.5. Test of the Catalytic Activity of Pd/$TiO_2$.* The Heck reactions of ArBr with styrene (Scheme 2) were carried out in a carousel (Radley's, UK), 12-port reaction under magnetic stirring at 600 rpm.

*2.6. General Procedure for the Catalytic Tests.* 1 molar equivalent of a base with respect to ArBr was transferred to a tube followed by 4 mL solvent and 0.25 mL of *n*-decane as a GC internal standard. 12 mmol, 1.38 mL, of styrene was added followed by (10 mmol; 1.053 mL) of bromobenzene. 0.1 mL of the mixture was withdrawn and added to 1 mL of the solvent for GC-FID analysis at $T_0$. Pd/$TiO_2$ (0.05 mmol% with respect to ArBr) was added and the mixture placed on the carousel at 140°C for 6 h. After completion of reaction at time $T_6$, 0.1 mL of the crude product in 1.0 mL of the solvent was identified using GC-FID Varian CP 3900. Aliquots were removed from the reaction mixture with a filtering syringe and analyzed with an Agilent gas chromatograph (GC) equipped with a 30-m × 0.32 mm, 0.25 $\mu$m film, HP-5 capillary column, and a FID detector. The GC program was as follows: initial temperature: 100°C, dwell time: 2 min, ramp: 10°C min$^{-1}$, final temperature: 300°C, and dwell time: 5 min. Conversion and selectivity were represented by product distributions (=relative area of GC signal) and GC yields (=relative area of GC-FID signals) referred to *n*-decane internal standard calibrated to the corresponding pure compound ($\Delta$rel < ±10%) and hence the percentage yield, TON, and TOF calculated relative to aryl halide. In separate control experiments, $TiO_2$ and $Pd(acac)_2$ were used as catalysts.

*2.7. Purification of the Product.* After completion of the reaction, 10 mL EtOAc was added to the vessel and the catalyst separated by simple filtration. Water 3 × 15 mL was added to the EtOAc phase and separated using a separating funnel. The organic layer was dried under low pressure and vacuum. The resulting crude product was purified by column chromatography using hexane: EtOAc (30 : 70) giving the pure product which was analyzed by NMR spectroscopy.

*2.8. Catalyst Optimization*

*Temperature Effects on Heck Reaction*. A temperature range of 80–140°C was used based on reported reaction temperature values obtained from literature [5].

*Base Effect on Heck Reaction*. $Na_2CO_3$, NaOAc, KOH, and $Et_3N$ were selected for screening, as they were found to be the most commonly used bases from literature. Selection of a base is necessary to ensure high turnover frequency for the catalyst and high product yields. Another experiment was carried out in the absence of a base.

*Solvent Effects on Heck Reaction*. The olefination of ArBr with styrene using Pd/$TiO_2$ and $Et_3N$ as base at 100°C was used to study the effect of various solvents. DMF, Toluene, MeOH, and EtOH were screened for the activity and selectivity in Heck reactions.

*Effect of Catalyst Loading*. The coupling of ArBr with styrene using DMF as solvent and NaOAc as base at 140°C was used to study the effect of various catalyst loading. The volume of the solvent, base, temperature, and time were kept constant. The experiments were repeated using 0.05, 00.1, 0.2, and 0.3 mol% Pd and the conversion was measured using GC-FID. In the control experiment, no catalyst was added.

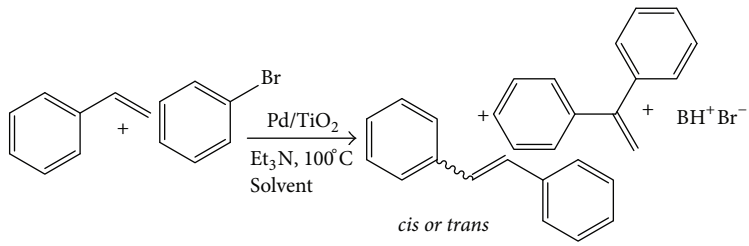


Scheme 2: Heck reaction.

*2.9. Recycling and Heterogeneity of the Catalyst*

*Recycling*. After the reaction was completed, the solid catalyst $Pd/TiO_2$ was first washed with dichloromethane to remove organic components. It was then with water to remove the base and salts. The catalyst was separated by centrifuging and finally washed with acetone to remove any adsorbed organic substrate, followed by drying at 120°C for 4 h as reported by Li and coworkers [12, 25].

*Heterogeneity Test*. To confirm whether the reaction took place on the surface or it leached, a hot filtration was carried out after 1 h and the progress of reaction was further monitored using GC-FID up to 6 h.

In an alternative method, the clear filtrate was collected in a glass vessel immediately after hot filtration, with careful evaporation to expel the organic compounds. The sample was then dissolved in 3 mL aqua regia, diluted to 10 mL, and the solution was filtered. The palladium content in solution was determined by ICP-OES, Spectro Arcos (Germany). Multiple analyses were applied for each sample for better accuracy.

*2.10. Percent Conversion of ArBr as Time Increases*. The general procedure described under Section 2.6 was followed. 2 ml samples were drawn from the reaction vessel after 10, 20, 30, 40, 50, 60, 120, 180, 240, 300, and 360 minutes and the product yields were analyzed using GC-FID.

## 3. Results and Discussion

Inspired by the reports of Obuya and her team in 2011, we electrospun $TiO_2$ NF and adsorbed Pd NPs on the fibers. Information about the surface was obtained from SEM images shown in Figure 1.

*3.1. SEM Analysis.* Figure 1(a) shows the PMMA/TIP NF after electrospinning, Figure 1(b) after hydrolysis, and Figure 1(c) after calcination. The fibers appeared smooth and had a diameter of 350 ± 50 nm. On calcination in air at 500°C, the NF diameters reduced to 180 ± 60 nm. On adding Pd NPs, the SEM images revealed small spots on the fibers representing palladium nanoparticles (Figures 1(d) and 1(e)).

*3.2. Elemental Analysis Using EDX.* The elemental composition of the as-synthesized $Pd/TiO_2$ was investigated by EDS and elemental mapping. The presence of various well-defined peaks of Pd, oxygen (O), and Ti confirmed the formation of $Pd/TiO_2$ (Figure 2(a)). The presence of the carbon peaks could be attributed to residual organics from the incomplete combustion of PMMA during calcination and the carbon that was coated on the fibers.

To confirm the distribution of Pd, O, and Ti ions onto the lattice surface, elemental mapping of the area is shown in Figure 2(b). The analysis shows that Pd, O, and Ti are distributed over the whole material, which further confirmed the formation of a moderately dispersed $Pd/TiO_2$. (yellow for Pd and blue for $TiO_2$).

*3.3. Confirmation of Absence of Organic Polymer in $TiO_2$ Nanofibers Using FTIR.* Figure 3 shows the FT-IR spectra of the PMMA, PMMA-TIP, and calcined $TiO_2$ recorded on Perkin–Elmer 100 spectrophotometer FTIR series (Tokyo, Japan).

The PMMA spectrum, Figure 3(b), showed peaks at 1140 $cm^{-1}$–1,270 $cm^{-1}$ (C–O–C str), 1385 $cm^{-1}$ and 741 $cm^{-1}$ ($\alpha$-$CH_3$), 836 $cm^{-1}$ (acrylate carboxyl group), and 3,436 $cm^{-1}$ and 1,634 $cm^{-1}$ (–OH str) indicating PMMA.

The PMMA/TIP fibers, Figure 3(c), showed peaks at 593 $cm^{-1}$ (Ti–O str), ~987 $cm^{-1}$ (O–O str), the sharp 1443 $cm^{-1}$ (latt vibrations of $TiO_2$), 1627 $cm^{-1}$ OH bend for $H_2O$ and Ti–OH, and 3436 and 1634 $cm^{-1}$ ($H_2O$ and Ti–OH) indicating $TiO_2$ [26]. This confirmed the presence of TIP in PMMA. Figure 3(b) shows the $TiO_2$ spectrum. The removal of PMMA during calcination was confirmed by the absence of $CH_x$ bending and stretching modes and presence of Ti–O stretch at ~600 $cm^{-1}$ in the $TiO_2$ spectrum.

*3.4. TEM Analysis of $Pd/TiO_2$ Catalyst.* Further morphological characterization of the synthesized catalyst was done using TEM. The deposition of Pd on $TiO_2$ was as shown in Figure 4.

The surface of the NF has dark shades representing the denser Pd NPs with estimated diameters of between 10 nm and 40 nm while the light shade is for the less dense $TiO_2$. The calcined fibers had a diameter of 180 ± 60 nm. On zooming in on Pd NPs at lower magnification, the Pd NPs were not well resolved. A few of the Pd particles were completely inside the NF, while some others were partially inside and partially outside the NF to some extent. TEM images were a proof of the successful nucleation and particle deposition on porous $TiO_2$ surface.

*3.5. XRD Analysis.* Figure 5 shows the XRD pattern of the calcined sample at 500°C in air for 4 h. ICDD database

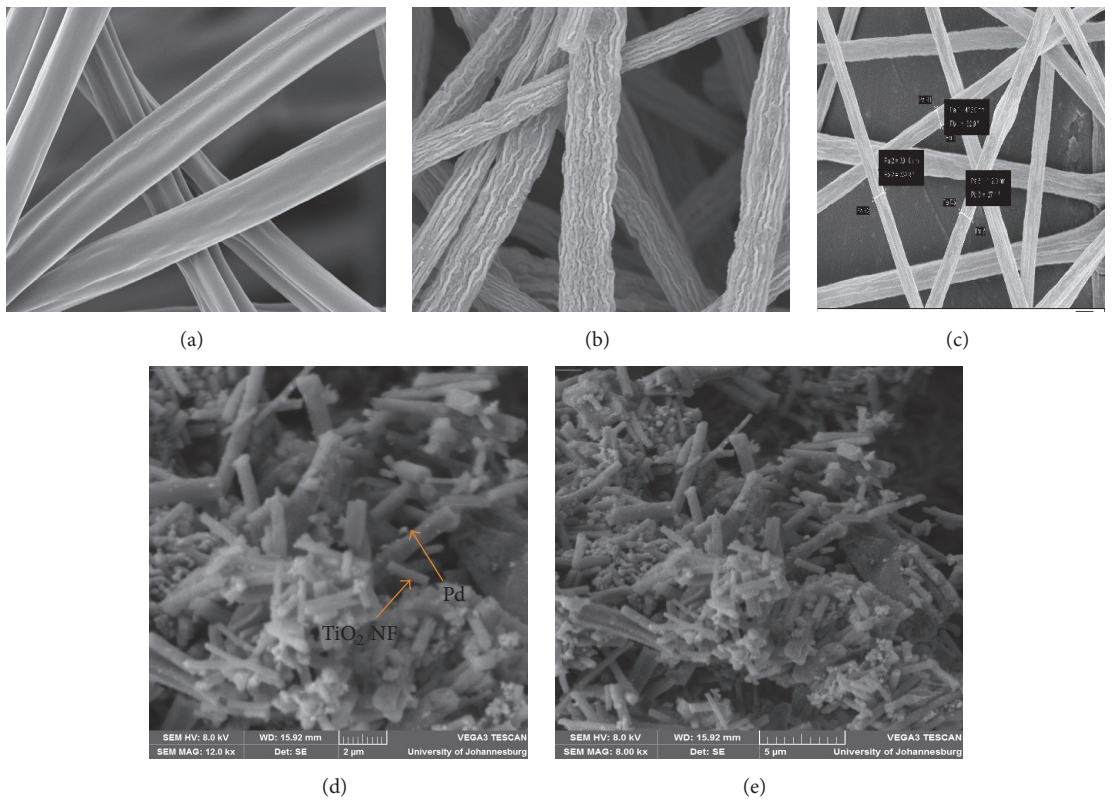


Figure 1: SEM images for (a) PMMA, (b) PMMA/TIP before calcination, (c) PMMA/TIP after calcination, (d) Pd/$TiO_2$ at 12.0 kV, and (e) Pd/$TiO_2$ at 8.0 kV.

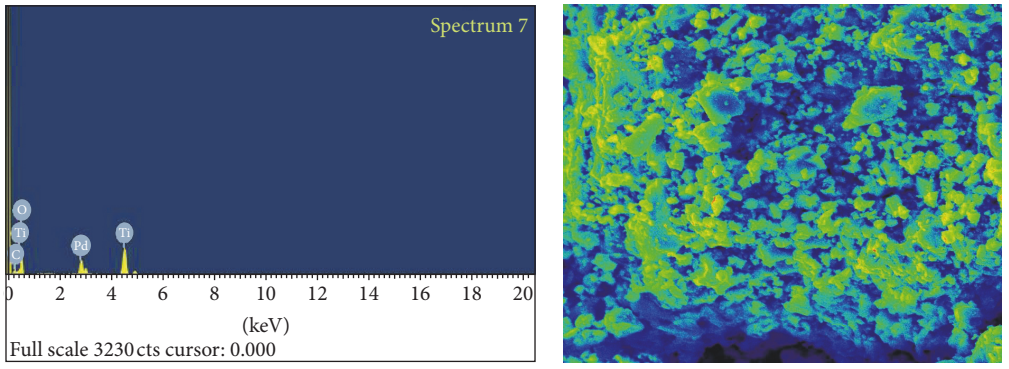


Figure 2: (a) EDAX image for Pd/$TiO_2$; (b) distribution of Pd, O, and Ti on to the lattice surface.

was used to identify the phases in the sample material. The diffraction patterns of the phase correlate well with the standard peaks (ICDD 01-075-2547). The peaks at 25.3 (101), 48.0 (200), 53.9 (105), and 62.4 (204) confirm the structure of anatase. The crystal structure was tetragonal with 141/amd space group [13, 27].

The average crystal size was significantly changed due to the addition of Pd NPs. The XRD reveals a Pd peak at $2\theta$, 40.4°, and some PdO at 33.5° [27]. Comparing $TiO_2$ to Pd/$TiO_2$, the peak widths in Pd/$TiO_2$ increased, implying particle size reduction due to formation of Pd/$TiO_2$.

*3.6. BET Analysis.* The BET surface area calculated from the monolayer of the nitrogen gas adsorbed was determined to be 53.4 $m^2$/g for $TiO_2$ and 43.4 $m^2$/g for Pd/$TiO_2$, the difference indicating the filling up of the pores. The isotherm plots revealed a type IV hysteresis loop with capillary condensation occurring in the pores. Per IUPAC classification, the results

Table 2: Pd-$TiO_2$ catalyzed Heck reaction of bromobenzene and styrene.

| Entry | Base | Solvent | Cat (Pd, mol%) | Temp (°C) | Time (h) | Conversion |
|---|---|---|---|---|---|---|
| (1) | $Et_3N$ | Toluene | 0.05 | 140 | 6 | 19 |
| (2) | $Et_3N$ | MeOH | 0.05 | 140 | 6 | 11 |
| (3) | $Et_3N$ | EtOH | 0.05 | 140 | 6 | 17 |
| (4) | $Et_3N$ | DMF | 0.05 | 140 | 6 | 33.9 |
| (5) | $K_2CO_3$ | DMF | 0.05 | 140 | 6 | 30.1 |
| (6) | NaOAc | DMF | 0.05 | 140 | 6 | 41.9 |
| (7) | $Na_2CO_3$ | DMF | 0.05 | 140 | 6 | 27.3 |
| (8) | NaOAc | DMF | 0.05 | 140 | 6 | 41.9 |
| (9) | NaOAc | DMF | 0.1 | 140 | 6 | 61.2 |
| (10) | NaOAc | DMF | 0.2 | 140 | 6 | 89.7 |
| (11) | NaOAc | DMF | 0.2 | 100 | 6 | 56.3 |
| (12) | NaOAc | DMF | 0.2 | 120 | 6 | 73.0 |
| (13) | NaOAc | DMF | 0.2 | 140 | 6 | 89.0 |
| (14) | NaOAc | DMF | 0.3 | 140 | 6 | 89.0 |
| (15) | — | DMF | 0.2 | 140 | 6 | 0 |
| (16) | NaOAc | DMF | — | 140 | 6 | 0 |
| (17) | NaOAc | DMF | $TiO_2$ | 140 | 6 | 3 |
| (18) | NaOAc | DMF | $Pd(acac)_2$ | 140 | 6 | 14 |

Reaction conditions: styrene (1.2 mmol), bromobenzene (1.0 mmole), base (1.0 mmole), and solvent (4 mL) based on average results (reaction carried out thrice for reproducibility).

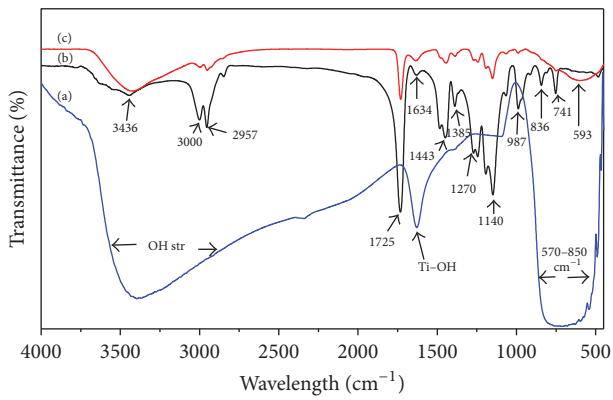


Figure 3: IR spectra of $TiO_2$ (a), PMMA (b), and PMMA/TIP (c) $TiO_2$.

gave a typical type IV isotherm, Figure 6(b). The hysteresis loop suggests mesoporous structure with pore condensation at high pressure.

The BJH single point pore volume was 0.170926 $cm^3/g$ and pore size was 12.7873 nm (Figure 5(a)).

The porosity and total intrusion volume for the synthesized 1 wt% Pd/$TiO_2$ sample were 34.52% and 0.17 mL/g. A comparison between these values and porosity (44.27%) and total intrusion volume (0.19 mL) for $TiO_2$ doped indicates a decrease in porosity and total intrusion volume. This indicates that the catalysts were mostly dispersed on the surface of the $TiO_2$ instead of also being embedded within the pores of $TiO_2$.

In comparison with what was reported by Wojcieszak and his group, the BET surface area obtained was much higher. Wojcieszak's group prepared Pd/$TiO_2$ using different methods (wet-impregnation, sol-gel, hydrazine reduction, and reverse microemulsion) and obtained very low surface areas (8-9 $m^2/g$) [28]. Obuya and her team did apply electrospinning in preparing the same catalyst and obtained a catalyst with a surface area of 93 $m^2/g$ which was quite high compared to the one reported in this thesis. This implied that electrospinning is a superior method for preparing high surface area NF. The difference between the surface area obtained by Obuya and her group and what is reported here could have resulted from local improvisations made on the electrospinning apparatus, lack of a pump, and use of glass Pasteur pipettes. Another reason could have been because of Pd NP preparation method and average molecular weight of the polymer [22].

*3.7. Catalyst Application.* Coupling reaction between ArBr and styrene was chosen as a model reaction (Scheme 2). The Pd/$TiO_2$ supported catalyst was prepared as described in the experimental section and was used as-synthesized. The catalytic data for Pd/$TiO_2$ are displayed in Table 2.

*3.8. Effect of Base.* $Et_3N$, an organic liquid base, was used with variable solvents (Toluene, MeOH, EtOH, and DMF) in the presence of 0.05% Pd loading. $Et_3N$ gave a higher conversion [12] with DMF as the solvent (Table 2, entry (4)). This is in agreement with what is reported in literature; the rates of reaction have been found to be faster in polar aprotic solvents (DMF) than in polar protic (MeOH, $H_2O$ and EtOH) and nonpolar solvents like Toluene [29]. This could be attributed to the fact that polar protic solvents are favourable for SN1 substitution reactions and hence will consume the

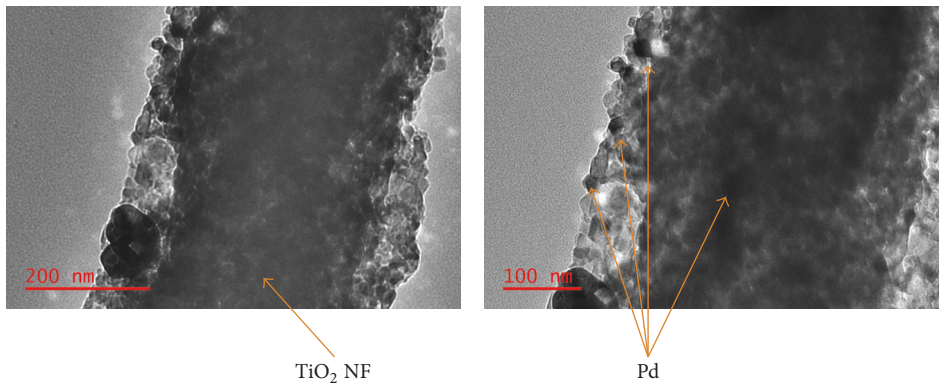


Figure 4: TEM images for $Pd/TiO_2$.

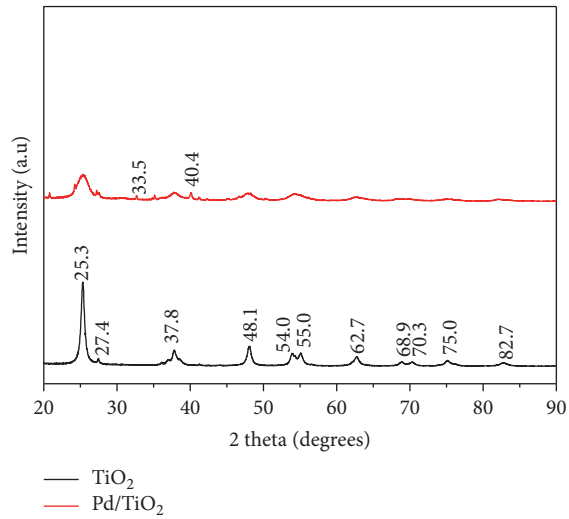


Figure 5: XRD spectra for $TiO_2$ and $Pd/TiO_2$ calcined samples at 500°C.

strong bases in a side reaction. On the other hand, polar aprotic solvents are favourable for SN2 substitution reactions, believed to be taking place in the proposed mechanism hence higher product yields [22].

*3.9. Effect of Bases.* Based on literature survey, $K_2CO_3$, NaOAc, $Na_2CO_3$, and $Et_3N$ bases were selected for screening. NaOAc improved yields in the presence of the polar DMF (Table 2, entry (6)). Inorganic bases recorded poor yields due to relative insolubility effects of the inorganic bases in the organic reaction matrix [13]. There was no conversion achieved when the reaction was carried out in the absence of a base. This indicates that removal of base from the reaction media inhibits the HR mechanism. It was suggested from an early point of HR mechanism that bases were needed to deprotonate the hydridopalladium complex formed at the $\beta$-elimination step in order to regenerate Pd(0). Li and his group used NaOAc as a base in their experiments and obtained 78% conversion [12].

*3.10. Effect of Catalyst Loading.* The catalytic activity of the system was investigated by varying the amount of catalyst. It was observed that 0.2 mol% (with respect to ArX) was sufficient for near completion giving a yield of 89.7% (Table 2, entry (13)). The effect of $TiO_2$ and $Pd(acac)_2$ as individual catalyst for the same reaction was also carried out and the result showed formation of a coupling reaction product in low yields (Table 2, entry (17) and entry (18)). This proves a synergistic effect of Pd and $TiO_2$ ($Pd/TiO_2$) NPs for enhancement of coupling yields in heterogenous system. No conversion was achieved when no catalyst was added to the reaction vessel.

*3.11. Effect of Temperature.* No conversion was achieved when the reaction was carried out at room temperature, but as the temperature increased, the reaction rate increased (Table 2, entries (11)–(13)). The conversion increased from 56.3 to 89.0% under the same reaction time. An increase in temperature was accompanied by an increase in the reaction rate due to increase in average kinetic energy of molecules and more collisions per unit time. The catalyst exhibited stability at high reaction temperatures up to 140°C. This can be attributed to the thermal stability of $TiO_2$ support and thus enhanced catalyst activity at high reaction temperatures. Homogenous Pd complexes will not be thermally stable at these temperatures [30].

*3.12. Catalytic Properties.* The synthesized $Pd/TiO_2$ catalyst exhibited high activity and selectivity in the Heck reaction of ArBr with styrene (Scheme 1). *E*-stilbene was observed as the main product in all cases.

A typical spectrum is given in Figure 6. The retention time of the chemical compounds in this experiment is STY (12.3 min), ArX (13.5 min), and stilbene (26.7 min) (Figure 7). The products were identified by GC-FID Varian 3900 series.

The catalyst was found to be highly active under air with reaction temperatures up to 140°C. Optimized reaction condition resulted in 89.7% conversions with a TON of 1993.4 and TOF value of 332.2 $hr^{-1}$.

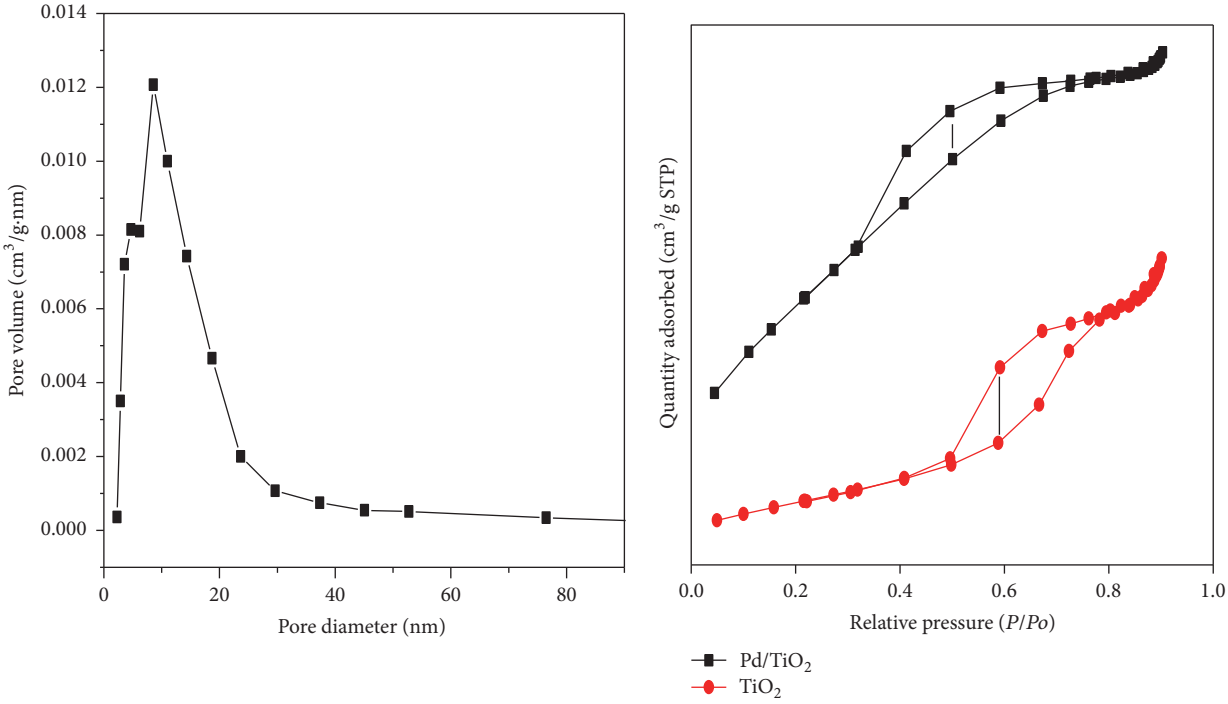


FIGURE 6: (a) BJH pore volume plot. (b) Nitrogen adsorption/desorption isotherms.

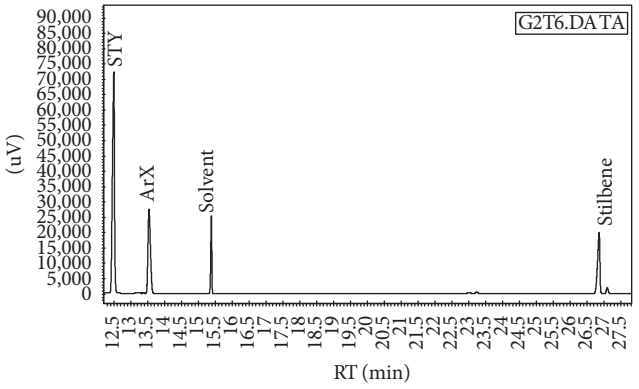


FIGURE 7: GC spectrum of reaction mixture.

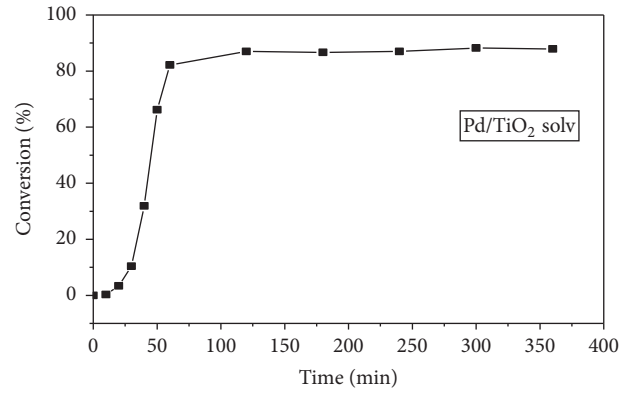


FIGURE 8: Product yield per given time.

*3.13. Heck Product Identification.* All the products are known compounds and the spectral data and melting points were identified by comparing with those reported in literature.

*3.14. E-Stilbene.* Analytical data: m.p.: 118°C; $^1$H NMR: $CDCl_3$, 400 MHz: 7.52 (d, $3J$ = 7.0 Hz, 4H, ortho-vinyl-$C_6H_5$); 7.36 (t, $3J$ = 7.5 Hz, 4H, meta-vinyl-$C_6H_5$); 7.27 (t, $3J$ = 7.0 Hz, 2H, para-vinyl-$C_6H_5$); 7.12 (s, 2H, CH-vinyl). $^{13}$C NMR: $CDCl_3$, 400 MHz: 137.36 (C-vinyl-$C_6H_5$); 128.67 (meta-vinyl-$C_6H_5$); 128.67 (CH-vinylic); 127.61 (para-vinyl-$C_6H_5$); 126.53 (ortho-vinyl-$C_6H_5$). $C_{14}H_{12}$-elemental analysis: Found (calc.): C 92.01 (93.29), H 6.64 (6.71).

*3.15. Percent Conversion of ArBr as Time Increases.* Time dependence of the yield under the optimized condition was studied. The reaction of ArBr with styrene came to near completion after 100 minutes (Figure 8).

The conversion was a bit slow in the first 15 minutes during induction period after which there was a gradual rise in the conversion up to about 83%. The conversion improved to 89.7% in the second hour and remained almost the same for the next 4 h. This implies that the conversion occurs in the first 60 minutes.

*3.16. Separation, Recycling, and Reuse.* Generally, the recycled catalyst Pd/$TiO_2$ showed high activity as in the first run

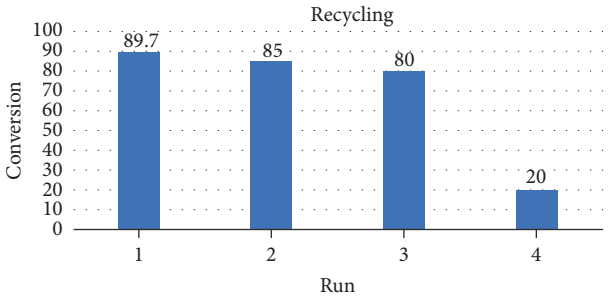


Figure 9: Recycling and reuse of selected $Pd/TiO_2$ catalysts in the Heck reaction of bromobenzene with styrene.

(Figure 9) and even a slightly increased activity after two runs.

In the first cycle, the coupling product was obtained with a yield of 89.7%. After the products and residual reactants were extracted, new starting materials were added to the remnant that contained the catalyst from the first reaction. After stirring for another 6 h at 140°C, the product yield was 85% in the second cycle. Similarly, the third cycle afforded a yield of 80%, and the subsequent fourth cycle afforded a 20% yield. The yield of the fourth cycle decreased greatly when comparing with the first cycle probably due to the conglomeration of particles and loss of the catalyst. The recycling could have also been hampered by partial structural damage to support and deactivation by coke deposition as also reported by Dams and his team (Dams et al., 2002). There was also observed increase in mass of the solid due to the presence of the catalyst, solid base, and salt making reproducibility difficult after every run. In addition to that, washing with water after separation reduced the activity of the catalysts. Filtering also leads to loss of some catalyst material.

*3.17. Pd Leaching Using Hot Filtration Test.* Figure 10 shows the progress of the reaction after removal of the catalyst.

There is very minimal noticeable change in the % conversion as the reaction progresses. This implied that minimal or no leaching occurred in the reaction. The activity reported in this paper could therefore be assumed to have arisen from the adsorbed Pd metal particles on the exterior surface of the $TiO_2$ NF, with more effective filling of the pores within the $TiO_2$ support. A hot filtration test proved the heterogenous nature of the supported catalyst and without a measurable homogenous contribution.

*3.18. Metal Leaching and the Nature of Catalysis.* Table 3 gives the results of catalyst leaching in the Heck coupling reaction of ArBr and styrene with 1.6% Pd at 140°C. According to the ICP-OES analysis, the Pd content of the heterogenous catalyst was determined to be 1.87 $mmol/g^{-1}$. The soluble Pd amount was found to range within 1.9–2.5 ppm in the reaction mixture which meets the requirements of less than 5 ppm residual heavy metal in product streams in the pharmaceutical industry [31]. The percentage of Pd leaching/Pd loading was around 1.2%. The soluble leached Pd could

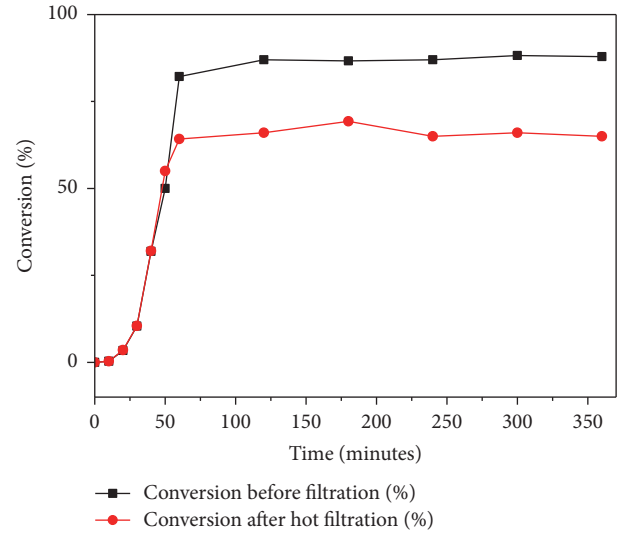


Figure 10: Effect of removing Pd catalyst from reaction after 100 minutes.

Table 3: Results of catalyst leaching.

| Catalyst | Cycles | Conversion (%) | Pd leaching (ppm) |
|---|---|---|---|
| $Pd/TiO_2$ | 1 | 87 | 2.5 |
| | 2 | 87 | 2.2 |
| | 3 | 86 | 1.9 |

likely be responsible for catalysis in Heck coupling reaction of ArBr and styrene. Pd leaching correlates significantly with the progress of the reaction, the nature of the starting materials and products, solvent, base, and atmosphere. These results agree with Shmidt and Mametova's observation of the oxidative attack of the halide to the metal crystallites, yielding directly Pd(II) in solution [32]. As indicated in previous literature reports, presence of Pd(II) ions in the reaction mixture indicates the $Pd/TiO_2$ catalyst is quasi-homogenous [11].

Comparable results were obtained by Nasrollahzadeh and coworkers in 2014. Nasrollahzadeh's group prepared 1% $Pd/TiO_2$ from commercial $TiO_2$. Pd NPs of diameter 40 nm were dispersed on the $TiO_2$ using simple drop drying process. The catalyst was found effective in ArI (1.0 mmol)-STY (1.5 mmol) HR coupling using $Et_3N$ base (2.0 mmol) and DMF solvent (4 mL) at 140°C for 24 h, giving 93% conversion. 0.2 ppm Pd was leached during the reaction. However, the dispersion of the Pd NPs was not reported by the group. They also carried their experiment under nitrogen.

In this paper, $TiO_2$ NF were prepared through electrospinning and $Pd(acac)_2$ precursor was used to deposit Pd NPs of ~12 nm on the NF through deposition-reduction method. The catalyst was found effective in ArCl (0.2 mmol)-STY (1.2 mmol) HR coupling using NaOAc base (2.0 mmol) and DMF solvent (4 mL) at 140°C for 6 h, giving 89.7% conversion. 2.2 ppm Pd was leached during the reaction.

The differences in the % conversion for the experiments could have been attributed to the differences in the bases used, the atmosphere in which the experiment was carried out, the hours the reaction took, the method of preparing the catalyst, the catalyst loading, and moles of styrene used with respect to ArX. While our team carried out the reaction under air, Nasrollahzadeh worked under nitrogen inert atmosphere. This probably hindered the recycling of the catalyst due to ease in agglomeration of Pd NPs. It is noted that the amount of Pd leached in our experiment was higher. Less Pd was leached in the Nasrollahzadeh probably due to effective filling of the pores in the catalyst than the one reported in this paper. Lastly, Nasrollahzadeh's group allowed the reaction to run for longer hours (24 h) allowing more time for more Pd NPs to be reused in the mechanism.

In 2011, Obuya and coworkers used photo-deposited Pd NPs of diameter 2–5 nm on electrospun $TiO_2$ NF of diameters $150 \pm 50$ nm. The product yield was 93% at optimized conditions and it had a TOF of 7.85 $min^{-1}$ [22]. Although our group used an approach almost like the approach of Obuya and her team, the percentage conversion obtained for the coupling of ArBr-STY in this paper was slightly lower (93% versus 89.7%). This was probably due to the catalyst prepared by Obuya and her group having $TiO_2$ NF having a higher surface area (93 $m^2/g$ versus 53 $m^2/g$) and use of a phase transfer salt during the coupling reaction. Another reason could be the differences in Pd particle size (2–5 nm versus 10–40 nm) and the distribution of Pd NP on the $TiO_2$ NF. In this paper, it was observed that the Pd NPs were not as evenly distributed as in Obuya's case.

*3.19. Mechanism.* Upon heating, electrons from $TiO_2$ NF are excited from the valence band into the unoccupied conduction band and positive holes are formed in the conduction band. These electrons from the conduction band can easily transfer to the Pd NPs surface generating electron heterogeneity at the $Pd/TiO_2$ surface. Thus, it is reasonable to expect the Pd sites with the energetic electrons at the $Pd/TiO_2$ surface will exhibit superior catalytic activity to that of palladium salt or $TiO_2$ alone. The ArBr is oxidatively added to the palladium to form a coordinatively unsaturated Pd complex—a characteristic of many coupling reactions. A π-complex is then formed by association with the electron rich alkene, leading to the formation of a new C–C bond. $\beta$-hydride elimination occurs to form product. The catalytic active Pd species is regenerated in the presence of NaOAc base and is recycled in a similar reaction cycle.

*3.20. Heck Cross-Coupling Reaction of ArBr and Methyl Acrylate.* The optimum conditions identified were employed in the coupling reaction of ArBr with methyl acrylate in the presence of the synthesized catalyst, $Pd/TiO_2$ (see Scheme 3).

ArBr and methyl acrylate went to completion giving a % conversion of 80.6. The product was identified as *E*-methyl cinnamate.

*E-Methyl Cinnamate.* $^1$H NMR (400 MHz, $CDCl_3$): $\delta$ 7.63 (d, $J$ = 16.0 Hz, 1H), 7.45 (dd, $J$ = 6.6, 3.0 Hz, 2H), 7.31 (dd, $J$ = 6.5, 3.7 Hz, 2H), 7.18 (s, 1H), 6.37 (d, $J$ = 16.0 Hz, 1H), 3.74 (s, 3H). $^{13}$C NMR (101 MHz, $CDCl_3$): $\delta$ 166.40, 143.85, 133.44, 129.27, 127.88, 127.05, 116.82, 50.66.

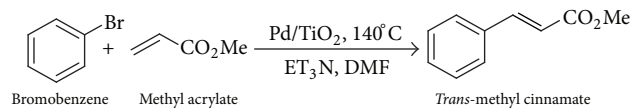


Scheme 3: Heck coupling of ArBr and methyl acrylate.

As seen in Table 1, Li and his coworkers are the only group that carried out this reaction using $Pd/TiO_2$. In the 2010, Li and his coworkers synthesized 0.1 to 0.5% $Pd/TiO_2$ by adsorption method by pH control and applied it in the Heck system of ArBr and methyl acrylate in the presence of 0.26% $Pd/TiO_2$ catalyst loading in the presence of KOAc and DMA gave 79% yield of product. Comparing the percent conversion for Li and his group and our group, there is only a slight increase in percentage conversion (79% versus 80.6%). Our results are in agreement with Li and his group [12].

## 4. Conclusions

$Pd/TiO_2$ catalyst prepared by electrospinning exhibits comparable activity and selectivity in the formation of carbon–carbon bonds by Heck reaction when compared to similar heterogeneous HR. Activated aryl bromides show a higher turnover at 140°C after few hours using the heterogeneous catalysts when compared to aryl chlorides. The activity of the catalysts can somehow be correlated with the nature of the support and the palladium dispersion and size. The catalysts can be recycled and reused with some significant loss of activity. The observed residual activity of the homogeneous solution after separation of the solid catalyst is found to be dependent on the filtration procedure, reaction condition, and dispersion of the metal on the support. Although there are several indications for a heterogeneous reaction mechanism, the participation of resolved Pd species (colloids or complexes) cannot be excluded.

These results reveal the potential of synthesized $Pd/TiO_2$ as efficient catalyst for industrial applications. The coupling reactions of aryl bromides with different olefins required higher temperature and extended reaction times. Optimized reaction condition resulted in 89.7% conversion with a TON of 1993.4 and TOF value of 332.2 $hr^{-1}$ for ArBr-styrene system and 79% TON 1044 and TOF 174 $hr^{-1}$ for ArBr-methyl acrylate system.

The method has the advantage of high yields, elimination of ligand and homogenous catalyst, simple methodology, and easy work up. The catalyst is eco-friendly and stable because it produces little waste and can be recovered and successfully reused without the significant loss of activity.

On atom economy, it is observed that all reagents and material used were incorporated into the final product. Secondly, we worked at relatively lower temperature and ambient pressure, which are both a factor for energy efficiency. Finally, unnecessary derivatization was avoided.

## Conflicts of Interest

The authors declare that there are no conflicts of interest regarding the publication of this paper.

## Acknowledgments

The authors are grateful to the NACOSTI for the ST&I Grant 5th CALL PhD/043, University of Johannesburg (UJ)-DFC and APK for laboratory use and material characterization; African-German Network of Excellence in Science (AGNES), the Federal Ministry of Education and Research (BMBF), and Alexander von Humboldt Foundation (AvH) for the grant to UJ; and the Catholic University of Eastern Africa (CUEA) and Kenyatta University (KU) for offering the laboratory space.

## References

[1] J. G. De Vries, "The Heck reaction in the production of fine chemicals," *Canadian Journal of Chemistry*, vol. 79, no. 5-6, pp. 1086–1092, 2001.

[2] R. F. Heck, R. F. Heck, and E.-U. Chimiste, *Palladium Reagents in Organic Syntheses*, vol. 179, Academic Press, London, UK, 1985.

[3] J. Tsuji, *Palladium Reagents and Catalysts*, Wiley and Sons, 1995.

[4] X.-F. Wu, P. Anbarasan, H. Neumann, and M. Beller, "From noble metal to Nobel Prize: palladium-catalyzed coupling reactions as key methods in organic synthesis," *Angewandte Chemie International Edition*, vol. 49, no. 48, pp. 9047–9050, 2010.

[5] A. Biffis, M. Zecca, and M. Basato, "Palladium metal catalysts in Heck C-C coupling reactions," *Journal of Molecular Catalysis A: Chemical*, vol. 173, no. 1-2, pp. 249–274, 2001.

[6] W. A. Herrmann, "N-heterocyclic carbenes: A new concept in organometallic catalysis," *Angewandte Chemie International Edition*, vol. 41, no. 8, pp. 1290–1309, 2002.

[7] R. N. Prabhu and R. Ramesh, "Catalytic application of dinuclear palladium(II) bis(thiosemicarbazone) complex in the Mizoroki-Heck reaction," *Tetrahedron Letters*, vol. 53, no. 44, pp. 5961–5965, 2012.

[8] W. Chen, R. Li, B. Han et al., "The design and synthesis of bis(thiourea) ligands and their application in Pd-catalyzed heck and suzuki reactions under aerobic conditions," *European Journal of Organic Chemistry*, no. 5, pp. 1177–1184, 2006.

[9] A. Corma, H. Garcia, and A. Leyva, "Catalytic activity of palladium supported on single wall carbon nanotubes compared to palladium supported on activated carbon: study of the Heck and Suzuki couplings, aerobic alcohol oxidation and selective hydrogenation," *Journal of Molecular Catalysis A: Chemical*, vol. 230, no. 1-2, pp. 97–105, 2005.

[10] I. Janowska, K. Chizari, J.-H. Olivier, R. Ziessel, M. J. Ledoux, and C. Pham-Huu, "A new recyclable Pd catalyst supported on vertically aligned carbon nanotubes for microwaves-assisted Heck reactions," *Comptes Rendus Chimie*, vol. 14, no. 7-8, pp. 663–670, 2011.

[11] K. Köhler, R. G. Heidenreich, J. G. E. Krauter, and J. Pietsch, "Highly active palladium/activated carbon catalysts for heck reactions: Correlation of activity, catalyst properties, and Pd leaching," *Chemistry - A European Journal*, vol. 8, no. 3, pp. 622–631, 2002.

[12] Z. Li, J. Chen, W. Su, and M. Hong, "A titania-supported highly dispersed palladium nano-catalyst generated via in situ reduction for efficient Heck coupling reaction," *Journal of Molecular Catalysis A: Chemical*, vol. 328, no. 1-2, pp. 93–98, 2010.

[13] M. Nasrollahzadeh, A. Azarian, A. Ehsani, and M. Khalaj, "Preparation, optical properties and catalytic activity of $TiO_2$@Pd nanoparticles as heterogeneous and reusable catalysts for ligand-free Heck coupling reaction," *Journal of Molecular Catalysis A: Chemical*, vol. 394, pp. 205–210, 2014.

[14] M. Wagner, K. Köhler, L. Djakovitch, S. Weinkauf, V. Hagen, and M. Muhler, "Heck reactions catalyzed by oxide-supported palladium - Structure-activity relationships," *Topics in Catalysis*, vol. 13, no. 3, pp. 319–326, 2000.

[15] L. Yin and J. Liebscher, "Carbon-carbon coupling reactions catalyzed by heterogeneous palladium catalysts," *Chemical Reviews*, vol. 107, no. 1, pp. 133–173, 2007.

[16] G. Durgun, Ö. Aksin, and L. Artok, "Pd-loaded NaY zeolite as a highly active catalyst for ligandless Suzuki-Miyaura reactions of aryl halides at low Pd loadings under aerobic conditions," *Journal of Molecular Catalysis A: Chemical*, vol. 278, no. 1-2, pp. 189–199, 2007.

[17] J. M. Calatayud, P. Pardo, and J. Alarcón, "Hydrothermal-mediated synthesis of orange Cr, Sb-containing TiO2 nanopigments with improved microstructure," *Dyes and Pigments*, vol. 139, pp. 33–41, 2017.

[18] S. Ogasawara and S. Kato, "Palladium nanoparticles captured in microporous polymers: A tailor-made catalyst for heterogeneous carbon cross-coupling reactions," *Journal of the American Chemical Society*, vol. 132, no. 13, pp. 4608–4613, 2010.

[19] K. Kaneda, M. Higuchi, and T. Imanaka, "Highly dispersed Pd on MgO as catalyst for activation of phenyl-chlorine bonds leading to carbon-carbon bond formation," *Journal of Molecular Catalysis*, vol. 63, no. 3, pp. L33–L36, 1990.

[20] R. L. Augustine and S. T. O'Leary, "Heterogeneous catalysis in organic chemistry Part 8. The use of supported palladium catalysts for the Heck arylation," *Journal of Molecular Catalysis*, vol. 72, no. 2, pp. 229–242, 1992.

[21] A. Wali, S. Muthukumaru Pillai, V. K. Kaushik, and S. Satish, "Arylation of acrylonitrile with iodobenzene over Pd/MgO catalyst," *Applied Catalysis A: General*, vol. 135, no. 1, pp. 83–93, 1996.

[22] E. A. Obuya, W. Harrigan, D. M. Andala, J. Lippens, T. C. Keane, and W. E. Jones Jr., "Photodeposited Pd nanoparticle catalysts supported on photoactivated TiO2 nanofibers," *Journal of Molecular Catalysis A: Chemical*, vol. 340, no. 1-2, pp. 89–98, 2011.

[23] S. J. Tauster, S. C. Fung, R. T. K. Baker, and J. A. Horsley, "Strong interactions in supported-metal catalysts," *Science*, vol. 211, article 4487, 1981.

[24] S. Chen, K. Huang, and J. A. Stearns, "Alkanethiolate-protected palladium nanoparticles," *Chemistry of Materials*, vol. 12, no. 2, pp. 540–547, 2000.

[25] K. Köhler, M. Wagner, and L. Djakovitch, "Supported palladium as catalyst for carbon-carbon bond construction (Heck reaction) in organic synthesis," *Catalysis Today*, vol. 66, no. 1, pp. 105–114, 2001.

[26] P. Gupta, C. Elkins, T. E. Long, and G. L. Wilkes, "Electrospinning of linear homopolymers of poly(methyl methacrylate): exploring relationships between fiber formation, viscosity, molecular weight and concentration in a good solvent," *Polymer Journal*, vol. 46, no. 13, pp. 4799–4810, 2005.

[27] B. C. E. Makhubela, A. Jardine, and G. S. Smith, "Pd nanosized particles supported on chitosan and 6-deoxy-6-amino chitosan as recyclable catalysts for Suzuki-Miyaura and Heck cross-coupling reactions," *Applied Catalysis A: General*, vol. 393, no. 1-2, pp. 231–241, 2011.

[28] R. Wojcieszak, R. Mateos-Blanco, D. Hauwaert, S. RG Carrazan, E. M Gaigneaux, and P. Ruiz, "Influence of the preparation method on catalytic properties of $Pd/TiO_2$ catalysts in the reaction of partial oxidation of methanol," *Current Catalysis*, vol. 2, no. 1, pp. 27–34, 2013.

[29] L. Djakovitch and K. Koehler, "Heterogeneously catalysed Heck reaction using palladium modified zeolites," *Journal of Molecular Catalysis A: Chemical*, vol. 142, no. 2, pp. 275–284, 1999.

[30] F. Zhao, K. Murakami, M. Shirai, and M. Arai, "Recyclable homogeneous/heterogeneous catalytic systems for heck reaction through reversible transfer of palladium species between solvent and support," *Journal of Catalysis*, vol. 194, no. 2, pp. 479–483, 2000.

[31] C. E. Garrett and K. Prasad, "The art of meeting palladium specifications in active pharmaceutical ingredients produced by Pd-catalyzed reactions," *Advanced Synthesis & Catalysis*, vol. 346, no. 8, pp. 889–900, 2004.

[32] H. Schmidt, G. Jonschker, S. Goedicke, and M. Mennig, "The Sol-gel process as a basic technology for nanoparticle-dispersed inorganic-organic composites," *Journal of Sol-Gel Science and Technology*, vol. 19, no. 1-3, pp. 39–51, 2000.